Electronic Supplementary Material (ESI) for Physical Chemistry Chemical Physics.
This journal is © the Owner Societies 2017

Electronic Supplementary Information

Ultrafast Coulomb Explosion of the Diiodomethane Molecule Induced by an X-ray Free-electron Laser Pulse

Tsukasa Takanashi,[a] Kosuke Nakamura,[b] Edwin Kukk,[c] Koji Motomura,[a]
Hironobu Fukuzawa,[a,d] Kiyonobu Nagaya,[d,e] Shin-ichi Wada,[d,f] Yoshiaki Kumagai,[a]
Denys Iablonskyi,[a] Yuta Ito,[a] Yuta Sakakibara,[a] Daehyun You,[a]
Toshiyuki Nishiyama,[e] Kazuki Asa,[e] Yuhiro Sato,[e] Takayuki Umemoto,[f]
Kango Kariyazono,[f] Kohei Ochiai,[b] Manabu Kanno,[b] Kaoru Yamazaki,[g,h]
Kuno Kooser,[c,i] Christophe Nicolas,[j] Catalin Miron,[j,k] Theodor Asavei,[k]
Liviu Neagu,[k] Markus Schöffler,[l] Gregor Kastirke,[l] Xiao-Jing Liu,[m]
Artem Rudenko,[n] Shigeki Owada,[d] Tetsuo Katayama,[o] Tadashi Togashi,[o]
Kensuke Tono,[o] Makina Yabashi,[d] Hirohiko Kono[b] and Kiyoshi Ueda*[a,d]

[a] Institute of Multidisciplinary Research for Advanced Materials, Tohoku University, Sendai 980-8577, Japan.

[b] Department of Chemistry, Graduate School of Science, Tohoku University, Sendai 980-8578, Japan.

[c] Department of Physics and Astronomy, University of Turku, Turku FI-20014, Finland.

[d] RIKEN SPring-8 Center, Sayo, Hyogo 679-5148, Japan.

[e] Department of Physics, Graduate School of Science, Kyoto University, Kyoto 606-8502, Japan.

[f] Department of Physical Science, Hiroshima University, Higashi-Hiroshima 739-8526, Japan.

[g] Department of Chemistry, Faculty of Science, Hokkaido University, Sapporo 060-0810, Japan.

[h] Institute for Materials Research, Tohoku University, Sendai 980-8577, Japan.

[i] Institute of Physics, University of Tartu, EST-50411 Tartu, Estonia.

[j] Synchrotron SOLEIL, L'Orme des Merisiers, Saint-Aubin, BP 48, FR-91192 Gif-sur-Yvette Cedex, France.

[k] Extreme Light Infrastructure - Nuclear Physics (ELI-NP), "Horia Hulubei" National Institute for Physics and Nuclear Engineering, 30 Reactorului Street, RO-077125 Măgurele, Jud. Ilfov, Romania.

[l] Institut für Kernphysik, J. W. Goethe Universität, Max-von-Laue-Str. 1, Frankfurt D-60438, Germany.

[m] School of Physics and Nuclear Energy Engineering, Beihang University, Beijing 100191, People's Republic of China.

[n] J. R. Macdonald Laboratory, Department of Physics, Kansas State University, Manhattan, Kansas 66506, USA.

[o] Japan Synchrotron Radiation Research Institute (JASRI), Sayo, Hyogo 679-5198, Japan.

*Corresponding author: Fax: +81-22-217-5380; Tel: +81-22-217-5381; E-mail: ueda@tagen.tohoku.ac.jp

1 Electric field effects of the XFEL pulse on electronic and nuclear dynamics

An effect of the XFEL electric field on the motion of nuclei to be explored is the time-dependent potential distortion induced by the XFEL electric field. The leading term of this additional force on the *j*th nucleus can be expressed by the optical cycle average term of the Raman type of interaction [S1,S2], such as $\boldsymbol{f}(t)\cdot\left(\partial\boldsymbol{\alpha}/\partial R_j\right)\cdot\boldsymbol{f}(t)/4$, where $\boldsymbol{f}(t)$ is the envelope vector of the XFEL electric field, $\boldsymbol{\alpha}$ is the polarizability tensor, and R_j is a Cartesian coordinate of the *j*th nucleus. This type of field-induced potential distortion accelerates the bond dissociation associated with H atoms or protons, because those species can move even in the short duration ~10 fs of the XFEL pulse. In the present SCC-DFTB approach, the effect of field-induced potential distortion is considered to be virtually included in the process of adding kinetic energy.

For the photon energy of 5.5 keV and the field strength of 1.5×10^{12} V/m, the ponderomotive radius of this strong XFEL electric field is only 3.8×10^{-5} Å and the ponderomotive energy is 1.5×10^{-3} eV. The effects of rescattering on the electronic and nuclear motion should be negligible.

2 On the accuracy of the SCC-DFTB method

We performed electronic structure calculations for potential surfaces of CH_2I_2 and CH_3I. The dissociation energy for C-I bond elongation of CH_3I is 3.7 eV for SCC-DFTB and 4.0 eV for B3LYP/6-311G(d,p); that for C-H bond elongation is 6.1 eV for SCC-DFTB and 6.9 eV for B3LYP/6-311G(d,p). The dissociation energy for C-I stretching of CH_2I_2 is 3.3 eV for SCC-DFTB and 3.6 eV for B3LYP/6-311G(d,p); that for C-H stretching is 5.7 eV for SCC-DFTB and 6.4 eV for B3LYP/6-311G(d,p). We obtained the same level of accuracy for monocation potential surfaces. We also compared the fragment charges calculated by the SCC-DFTB and B3LYP/6-311G(d,p). Both methods provide almost the same fragment charges; e.g. for CH_3I at the electronic temperature $T_e \approx 0$, the fragment charges of the iodine and carbon ions for $Q_{max} = 11$

was +5 and +3, respectively.

In the present SCC-DFTB/MD, no ionization energies are directly used; we merely switch the charge state of a molecule to the higher one according to the charge build-up curve eqn (1). We however carried out calculations on trial to confirm the accuracy of the SCC-DFTB method: The ΔSCF first ionization energy of CH_3I is 9.9 eV for SCC-DFTB and 9.8 eV for B3LYP/6-311G(d,p) (The experimental IP = 9.52 eV [S3]); The corresponding value of CH_2I_2 is 9.3 eV for SCC-DFTB and 9.4 eV for B3LYP/6-311G(d,p).

3 Optimal value of the charge build-up time τ

We examined how the calculated kinetic energies of fragment ions depend on the charge build-up constant τ. With increasing (decreasing) τ, the kinetic energy distribution of each fragment ion is shifted toward the lower (higher) energy side. For example, in the case of CH_2I_2, the average kinetic energy of iodine ions for $Q_{\mathrm{fin}} = 9$ is lower by 0.9 eV for $\tau = 15$ fs than for $\tau = 10$ fs; that of carbon ions is lower by 5.0 eV. For $\tau = 5$ fs, the average kinetic energy of iodine ions for $Q_{\mathrm{fin}} = 9$ is higher by 1.6 eV and that of carbon ions is higher by 6.1 eV, compared to the case of $\tau = 10$ fs. Since the kinetic energy distributions for iodine and carbon ions both shift to the same energy side irrespective of whether τ gets longer or shorter, more satisfactory results cannot be obtained by changing the value of τ. To obtain better agreement with the experimental results (See Figs. 5 and 6), $\tau > 10$ fs is desirable for carbon ions while $\tau < 10$ fs is desirable for iodine ions. We therefore determine the optimal τ in terms of the kinetic energy sum distributions of carbon and iodine ions. The deviations from the experimental results are then minimized around $\tau = 10$ fs for both CH_2I_2 and CH_3I, as shown in Fig. S1.

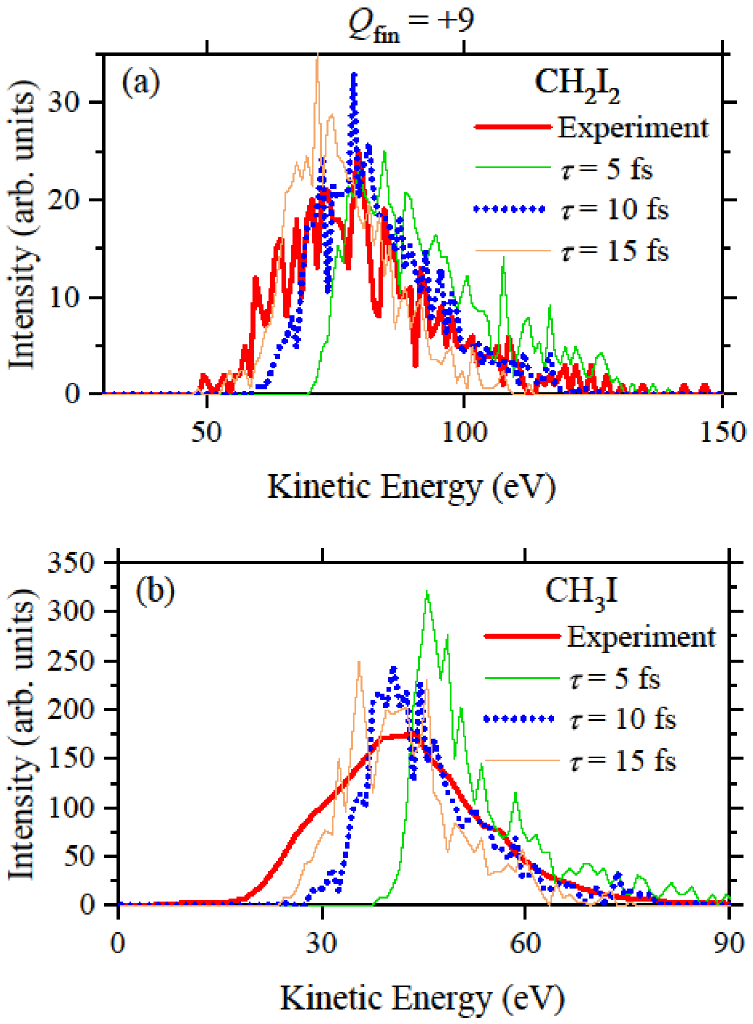

Fig. S1 Charge build-up time τ dependence of kinetic energy sum distributions of carbon and iodine ions for Q_{max} = 9: (a) CH_2I_2; (b) CH_3I.

4 Total amount of injected kinetic energy in the SCC-DFTB approach

We analyzed how much vibrational energy is injected by the time when the charge of the molecule reaches the theoretical final charge Q_{max}. As shown in Fig. S2, the average injection energy ΔE, defined by eqn (3), increases almost linearly with Q_{max}. ΔE increases by ~4 eV per unit increase in Q_{max}; for CH_3I, it is 21 eV at Q_{max} = 5 and 57 eV at Q_{max} = 14; for CH_2I_2, it is 23 eV at Q_{max} = 5 and 63 eV at Q_{max} = 14. The average injection energy per unit charge increase however gradually diminishes as Q_{max} increases, as shown in Fig. S2, because more bonds exceed the critical distance for energy injection. For the same Q_{max}, ΔE was a little larger for CH_2I_2 than for CH_3I because CH_2I_2 has two long lasting C-I bonds.

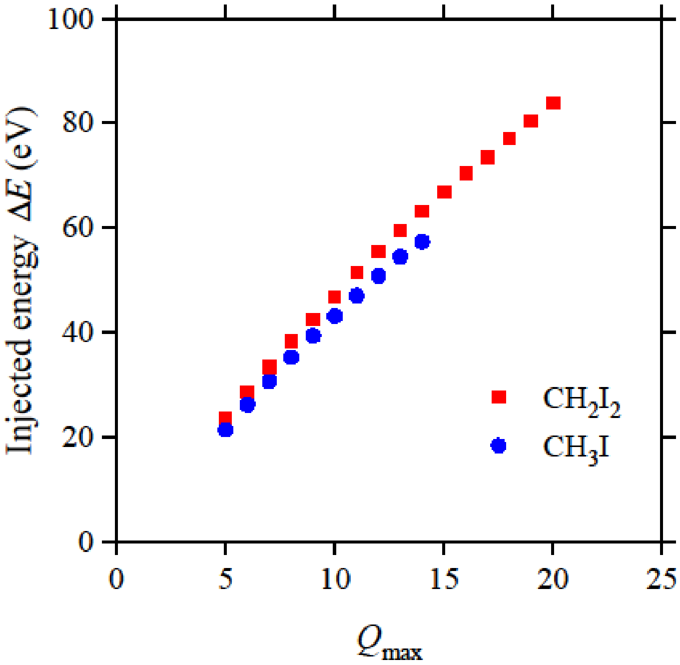

Fig. S2 Injected energy ΔE as a function of the final charge Q_{max}.

5 Role of the addition of repulsive kinetic energy

The ground state potential surfaces for highly charged CH_2I_2 or CH_3I are repulsive. The nuclei gain extra kinetic energies on those repulsive potentials. Assuming that the ground and excited state potentials are not be perfectly parallel to one another and there are chances of nonadiabatic transitions, we further added repulsive momenta for high charge states of $Q_{\mathrm{tot}}(t) \geq 8$, where all atoms have considerable positive charges (≥ 1). To examine the role of this extra addition of repulsive kinetic energy for $Q_{\mathrm{tot}}(t) \geq 8$, we compared the two cases with and without adding artificial kinetic energies for the final charges $Q_{\mathrm{max}} \geq 8$. For both molecules, the kinetic energy distributions of heavy iodine atoms in these two cases are nearly equal to each other; they have nearly the same shape and average kinetic energy. For carbon atoms, the kinetic energy distributions depend on the presence or absence of added repulsive kinetic energies for $Q_{\mathrm{tot}}(t) \geq 8$. At $Q_{\mathrm{max}} = 9$, the addition of extra kinetic energy for $Q_{\mathrm{tot}}(t) \geq 8$ change the kinetic energy distributions only slightly. The kinetic energy distribution of carbon ions for CH_2I_2 is sifted by 3.5 eV with adding extra kinetic energy when $Q_{\mathrm{tot}}(t) \geq 8$; that for CH_3I is shifted by only 0.5 eV. In the case of $Q_{\mathrm{max}} = 9$, most of the bonds exceed the critical distance for kinetic energy injection when $Q_{\mathrm{tot}}(t)$ reaches 8. The difference between the two cases becomes more distinct as Q_{max} increases. At $Q_{\mathrm{max}} = 14$, the kinetic energy distribution of carbon atoms for CH_2I_2 is sifted by 6.8 eV toward the higher energy side with adding extra kinetic energy when $Q_{\mathrm{tot}}(t) \geq 8$; that for CH_3I is shifted by 1.6 eV. The energy shift is more pronounced for CH_2I_2 than for CH_3I because CH_2I_2 has two heavy iodine atoms and expands slowly. These energy shifts are relatively small, since the average kinetic energy of carbon ions is beyond 100 eV: The addition of repulsive kinetic energies for $Q_{\mathrm{tot}}(t) \geq 8$ is not crucial at present. We however noted that the simulated kinetic energy distribution of carbon atoms becomes closer to the experimental one for CH_3I by the addition of extra kinetic energy for $Q_{\mathrm{tot}}(t) \geq 8$ and becomes worse for CH_2I_2. To obtain consistent agreement in kinetic energy distributions, it is necessary to scrutinize the physics behind the kinetic energy injection based on eqn (4) from the viewpoint of first-principles simulations.

References

S1 Y. Sato, H. Kono, S. Koseki and Y. Fujimura, *J. Am. Chem. Soc.* 2003, **125**, 8019-8031.

S2 N. Niitsu, M. Kikuchi, H. Ikeda, K. Yamazaki, M. Kanno, H. Kono, K. Mitsuke, M. Toda and K. Nakai, *J. Chem. Phys.* 2012, **136**, 164304.

S3 *"NIST Chemistry WebBook", NIST Standard Reference Database Number 69*, ed. P. J. Linstrom and W. G. Mallard, National Institute of Standards and Technology, Gaithersburg MD, 20899, http://webbook.nist.gov.